Influence of oxygen and argon ratio on electrical and physical characteristics of $Zr_xHf_{1-x}O_2$- based MOS devices

Rezwana Sultana[1,2,], Karimul Islam[1,2] and Supratic Chakraborty[1]*

[1]*Saha Institute of Nuclear Physics, 1/AF Bidhannagar, Kolkata 700 064, India*
[2]*Homi Bhabha National Institute, BARC Training School Complex, Anushaktinagar, Mumbai 400 094, India*

Email:rezwana.sultana@saha.ac.in

Abstract

In this work, $Zr_xHf_{1-x}O_2$ thin films were deposited on silicon substrate (*n*-type) using co-sputtering technique at various O_2/Ar ratios in the plasma. X-ray photoelectron spectroscopy (XPS) and scanning electron microscopy (SEM) technique have been employed to study the chemical composition and surface morphology of $Zr_xHf_{1-x}O_2$ thin films, respectively. Capacitance-voltage (*C*-*V*) and current-voltage (*I*-*V*) measurements have been performed to look on the electrical response of all the deposited thin films. Exploration of XPS data reveals that the number of defect states present in the film decreases with increasing oxygen flow rate. The SEM images confirm that surface roughness of the as deposited films enhance with the increasing grain size. From the C-V curve measured at 1 MHz frequency, oxide charge density (Q_{ox}) and interface charge density (D_{it}) have been calculated. The film deposited at O_2/Ar gas flow ratio of 1:3 gives higher value of Q_{OX} for smaller grain size. Structural reduction and lesser unsaturated bonds at the $Zr_xHf_{1-x}O_2$/Si interface cause the minimum D_{it} at a ratio of 1:5. Current-voltage (*I*-*V*) measurement indicates clearly that the leakage current decrease with increasing argon flow rate. Electrical properties and surface morphology of all the films were studied and a correlation has been made between the surface morphology and electrical properties of all the films.

Keywords: *RF reactive co-sputtering*, *X-ray photoelectron spectroscopy, Scanning electron microscopy, MOS device, thin film.*

1. Introduction

In recent times, fabrication of portable, high efficiency and low power consuming electronic devices at low cost is a great challenge for the researchers [1]. Research on different high-*k*based metal oxides such as Ta_2O_5, TiO_2, ZrO_2, HfO_2 are currently under consideration to full fill the requirement of the semi-conductor industry. HfO_2 and ZrO_2 are considered as a promising candidate because of relatively higher dielectric constant, wide band gap and high temperature stability [2]. Zirconium doped HfO_2 has numerous advantages. Physical and chemical properties of HfO_2 and ZrO_2 are very similar. Atomic radius of Hf and Zr are almost equivalent [3].

A ZrxHf1–xO2 film gives better stability with higher-*k* value than pure HfO_2. It also shows higher amorphous-to-polycrystalline transition temperature and low leakage current because atomic structure of Zr and Hf are comparable [4]. The morphological and structural properties of high-k dielectric thin films influence the electrical properties. So before finding its application in microelectronic devices, a correlation between morphological, structural and electrical properties is highly beneficial. In the present work, $Zr_xHf_{1-x}O_2$ films are deposited with reactive RF co-sputtering technique with various O_2/Ar ratios. A systematic investigation on the surface morphology and some careful electrical measurements has been done to establish a correlation between morphological and electrical properties of the films.

2. Experimental

$Zr_xHf_{1-x}O_2$ thin-films were deposited on *n*-type silicon substrates using reactive RF co-sputtering method at room temperature. Si (100) wafer of 1 cm^2 area having 1–10 Ω-cm resistivity was taken as substrate. The substrates were then cleaned using Radio Corporation of America (RCA)-based cleaning technique [5]. After that the substrates were rinsed into 1% HF solution for 1 min to take out stray oxides. All the substrates were then instantly loaded into the sputtering chamber. The base pressure $3x10^{-6}$ Torr of sputtered chamber has been reached using vacuum turbo pump which was backed by rotary pump. The deposition pressure has been kept at 5 mT during deposition. The required sputtering gas argon and reactive gas oxygen were introduced into the chamber by adjusting mass flow controller. Depositions were carried out for 40 min at room temperature with power applied to Zr target and Hf target were 4W and 50W, respectively. The films were deposited at four different O_2/Ar ratios. The ratios were 1:6, 1:5, 1:4 and 1:3. They are denoted as SR6, SR5, SR4 and SR3, respectively. Table 1 shows the summary of the deposition parameters used. To study the valance states of the elements present in the $Zr_xHf_{1-x}O_2$ thin-films, XPS technique has been performed at x-ray Photo-Electron Spectroscopy (PES) Beam line (BL-14) of Indus-2 at RRCAT-Indore, India. The energy of Indus-2 storage ring is 2.5 GeV. The base-pressure of the chamber is 5×10^{-9} mbar while the electron-beam energy was 4.4 keV. Scanning electron microscopy (SEM) has been used to study the surface morphology of all the films.

Table 1. Parameters used in sputtering during $Zr_xHf_{1-x}O_2$ films deposition.

Parameters	**Details**
Target	Hf, Zr (99.999% purity)
Power	50 W , 4W
Deposition duration	40 min
Flow rate ratio of O_2/Ar (sccm)	7:42 , 8: 40 , 10: 40 and 12: 36
Deposition temperature	Room temperature (~27˚C)

For electrical characterization metallic aluminium has been evaporated on all the samples using electron beam evaporation technique. Then 100 µm-diameter gate electrodes were patterned using UV photolithography technique to form Al/$Zr_xHf_{1-x}O_2$ /Si metal-oxide-semiconductor (MOS) structure. The capacitance–voltage (*C*–*V*) and leakage current–voltage (*I*–*V*) measurements of Al/$Zr_xHf_{1-x}O_2$/Si metal-oxide-semiconductor (MOS) devices have been measured by 4200-SCS semiconductor parameter analyzer equipped with PA-4200 pre-amplifiers.

3. Results and discussion

FIG 1. shows the schematic diagram of Al/ $Zr_xHf_{1-x}O_2$/Si device structure.

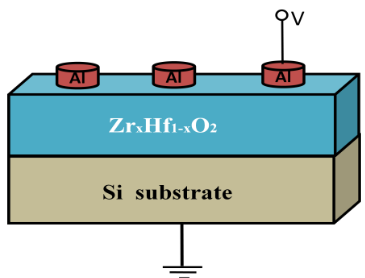

FIG 1. A schematic diagram of Al/ $Zr_xHf_{1-x}O_2$/Si device.

3.1 Chemical composition

The elemental composition and chemical state of $Zr_xHf_{1-x}O_2$ thin films were investigated by XPS measurement.

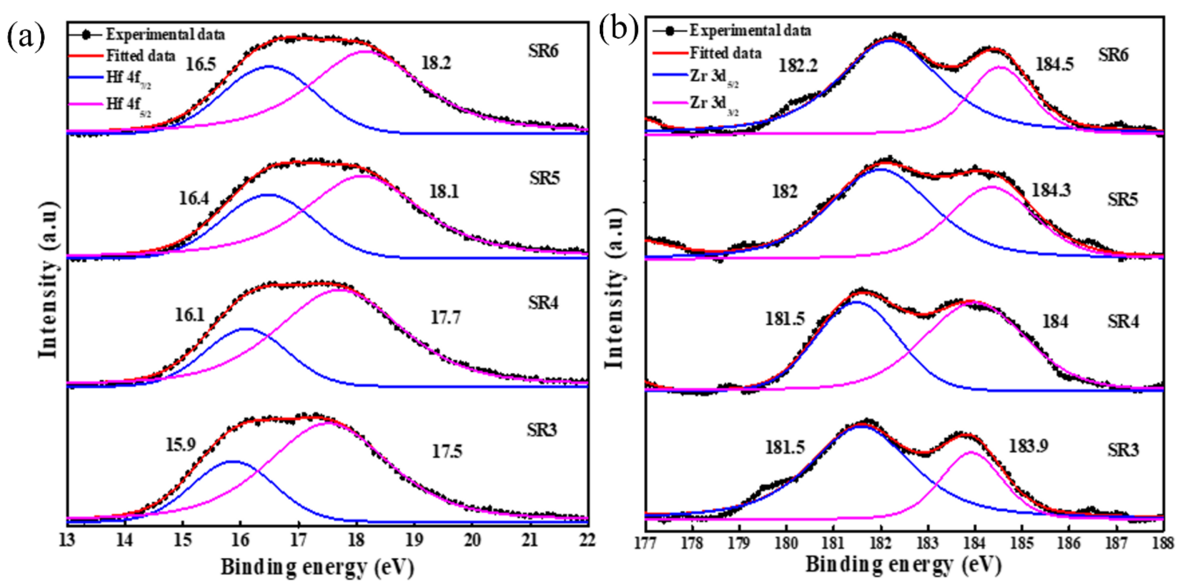

FIG 2. XPS spectra of (a) Hf 4f and (b) Zr 3d of $Zr_xHf_{1-x}O_2$ thin films with different O_2/Ar ratios.

The Hf 4f and Zr 3d XPS spectra of all the thin films deposited at different O_2/Ar ratio, calibrated from the C 1s peak at 284.8 eV, are shown in FIG 2. All the xps spectra is deconvoluted using casaXPS software. The binding energies of Hf $4f_{7/2}$ and Hf $4f_{5/2}$ of SR6 are 16.5 and 18.2 eV, respectively, indicating the formation of the Hf–O bond in the $Zr_xHf_{1-x}O_2$films. Similarly, the peaks arise at 182.2 and 184.5 eV in Zr 3d spectra indicates Zr $3d_{5/2}$ and Zr 3d $_{3/2}$, respectively. Difference of 2.3 eV between two peaks ensures complete oxidization of metallic Zr during sputtering [6]. XPS peaks of Hf 4f and Zr 3d shift to lower binding energy with increasing oxygen flow. Completely oxidized metal oxide has lower binding energy than that of oxygen deficient oxide. By increasing oxygen flow and reducing argon flow into the chamber the Hf and Zr density become relatively low and the collision of O_2 with Zr and Hf increase, which reduces the kinetic energy of particles. Thus, the combination of Zr and Hf with Oxygen becomes weaker. The XPS result shows that for SR6 the peak shifts to the higher BE that indicates more defects, generally oxygen vacancy exists in the film.

3.2 surface morphology

The grains are observed in the surface of all the films. Larger grains are found at higher argon and lower oxygen concentration in the plasma. This may be due to the enhancement in the sputter rate of hafnium and zirconium with higher argon concentration. Higher sputtering gas flow rate increases energy flux at the substrate which can enhance deposition rate and grain size. The introduction of O_2 gas into the deposition chamber increases the oxidation probability reducing deposition rate. With growing oxygen flow the sputtering plasma deteriorate and thus sputtering yield of target materials get reduced [7]. The SEM images of all the samples are shown in the FIG 3. The average grain size of SR6, SR5, SR4 and SR3 samples are 55 nm, 44 nm, 34 nm and 25 nm, respectively. So, it is clear that the XPS result support SEM analysis.

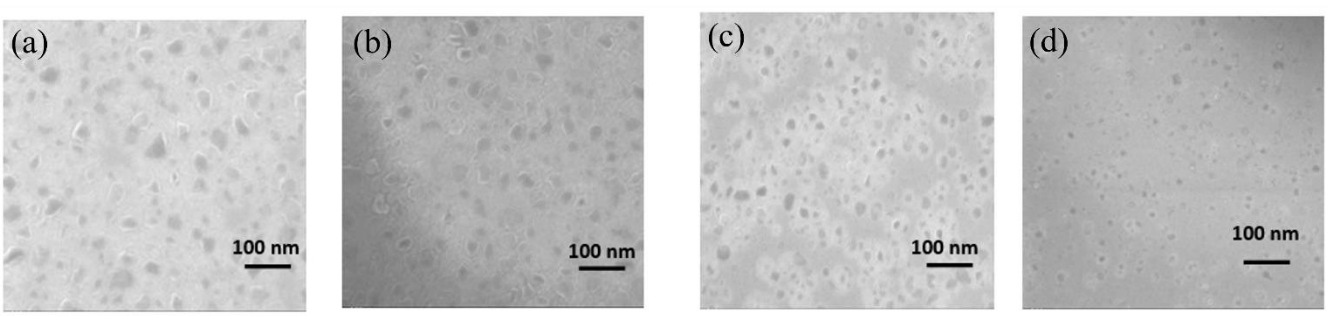

FIG 3. SEM images of $Zr_xHf_{1-x}O_2$ thin films grown at various O_2/Ar gas flow ratios a) SR6, b) SR5, c) SR4, d) SR3. The scale bar represents 100 nm.

3.3 Current - voltage characteristics

The variation of leakage current (I) with gate voltage (V) of all the samples are shown in FIG 4. The I−V measurements of Al/$Zr_xHf_{1-x}O_2$/Si-based MOS devices were carried out by applying positive bias on top electrode with the bottom electrode grounded. Positive bias voltage was swept from 0 to +12 V. At the lower bias, current increases rapidly and then it becomes quasi-saturated. There is also a slight variation in the leakage current with different O_2/Ar ratio. The value of the gate leakage current gets reduced from SR3 to SR6 with greater Ar flow in the plasma because larger grain size in surface contains less number of grain boundaries to allow current conducting path. Reported data confirms that large part of the leakage current is transported through grain boundaries [8].

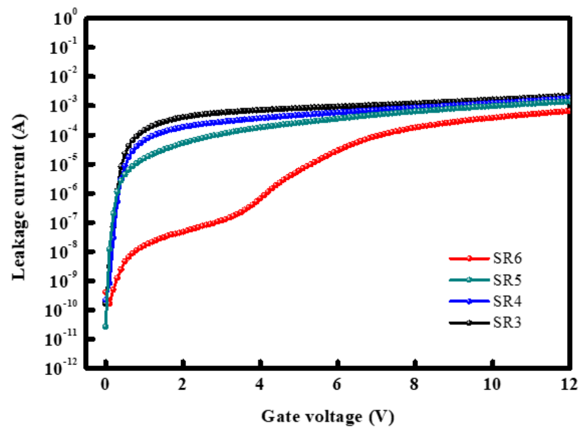

FIG 4. Variation of gate leakage current with applied voltage for all samples.

3.4 Capacitance-Voltage characteristics

The normalized C–V curves measured at 1 MHz of Al/$Zr_xHf_{1-x}O_2$/Si (MOS) based structures are plotted in FIG 5(a). Q_{ox}has been calculated from the flat band voltage shift, whereas D_{it} was calculated using Terman method with the help of C–V curves [9]. The variation of $Q_{ox}$and D_{it} with O_2/Ar gas flow ratio have been plotted in FIG 5(b). The oxide charge density increased with the decrease in the argon flow and increase in oxygen flow from SR6 to SR3 due to the decrease of the grain sizes. The various trap sites such as defects, voids, unsaturated bonds, impurities are usually exist at the grain boundaries. Large number of trapping centres are available in the films with smaller grains due to its large grain boundary surfaces. All the traps present in the films capture free carriers. With the decrease of granular sizes surface area of grain boundaries increase. Consequently, densities of the defect sites increase with the reduction in the average grain sizes [10]. An abrupt increase in the $D_{it}$was observed for SR6 having higher argon flow. The enrichment of dangling bonds, defect densities at the $Zr_xHf_{1-x}O_2$/Si interface are the causes of higher D_{it}.

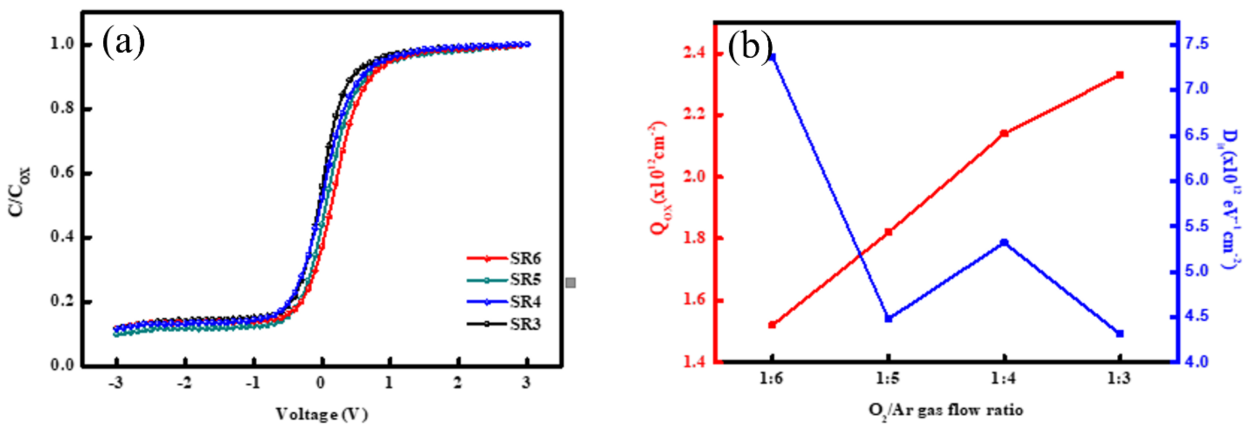

FIG 5. (a) Capacitance–voltage characteristics of $Zr_xHf_{1-x}O_2$ films grown at various O_2/Ar gas flow ratio (b) Variation of oxide and interface charge densities of $Zr_xHf_{1-x}O_2$ films with different O_2/Ar gas flow ratio.

4. Conclusion

Surface and electrical properties of the as deposited $Zr_xHf_{1-x}O_2$ films were studied in detail to establish a correlation between the morphological and electrical properties of the thin films. XPS and SEM technique have been employed to study the elemental composition and surface morphology of the films with different O_2/Ar ratios, respectively. XPS study reveals that there are no metallic Hf and Zr present in the films as they are fully oxidized and with increasing oxygen flow the defect density in the films reduces. As the grain size decreases the surface roughness of the as deposited films decreases. The oxide trap density found in $Zr_xHf_{1-x}O_2$ films depends on the O_2/Ar flow ratio. The SR6 sample has minimum Q_{ox}valued 1.52 x 10^{12} cm^{-2} due to the evolution of larger grains at film surface. The rise in D_{it} up to 7.37×10^{12} $eV^{-1}cm^{-2}$ for higher argon content is observed due to higher defect densities. Lowest leakage current is observed for SR6.

5. Acknowledgments

The authors gratefully acknowledged the technical and experimental support from Mr. Debraj Dey of Saha Institute of Nuclear Physics for SEM study. The author also would like to thank Mr. U.K. Goutam to provide XPS facility. The first author is thankful to Department of Atomic Energy (DAE), Government of India for financial support.

REFERENCES

[1] M H Huang, P C Fan and K H Chen, IEEE Trans. Power Electron. 24, 5 (2009)

[2] T R Shan, B D Devine, T W Kemper, S B Sinnott and S R Phillpot, Phys. Rev. B 81, 125328 (2010)

[3] J C Slater, J. Chem. Phys. 41, 3199 (1964)

[4] Y Kuo, J Lu, J Yan, T Yuan, H C Kim, J Peterson, M Gardner, S Chatterjee and W Luo, ECS Trans.1, 447-454 (2006)

[5] W Kern, J. Electrochem. Soc. 137, 1887–1889 (1990)

[6] X Wu, P Zhou, J Li, L Y Chen, H B Lv, Y Y Li and T A Tang, Appl. Phys. Lett. 90, 183507 (2007)

[7] M A Mansoori, S A Shaibani, A A Jaeedi, J Lee, D Choi and F S Hasoon, AIP Advances 7, 125105 (2017)

[8] J P Kar, S Mukherjee, G Bose, S Tuli and J M Myoung, Mater. Sci. Technol. 25, 1023 (2009)

[9] E H Nicolian and J R Brews, Metal, Oxide Semiconductor Physics and Technology (Wiley, New York) 325–426 (1982)

[10] J P Kar, G Bose and S Tuli, Curr. Appl. Phys. 6, 873–876 (2006)